JOURNAL OF MODERN OPTICS, 1996, VOL. 43, NO. 6, 1101–1110

The inverted surface plasmon resonance: Phenomenological explanation

E. POPOV, B. BOZKOV

Institute of Solid State Physics, Bulgarian Academy of Sciences, 72 Tzarigradsko Chaussee blvd., Sofia 1784, Bulgaria

and M. NEVIERE

Laboratoire d'Optique Electromagnétique, URA CNRS 843, Faculté des Sciences et Technique de St Jérôme, 13397 Marseille Cedex 20, France

(*Received 25 September 1995; revision received 17 November 1995*)

Abstract. A phenomenological explanation is made of different types of resonances in the reflectivity curves of a prism coupler in the region of surface plasmon excitation. The approach is based on the poles and zeros of the scattering operator and demonstrates that the existence of peaks instead of dips is natural and is determined by the positions of the pole and the zero in the complex plane.

1. Introduction

In 1993 Printz and Sambles [1] investigated surface plasmon excitation in prism couplers. Contrary to the common opinion that this phenomenon leads to sharp (resonance) minima in the reflectivity, they found a case when a well-defined maximum can be observed. The system under consideration is sketched in figure 1. It consists of a prism with its large facet covered with two layers of chromium and gold. Under specific conditions, a plane wave incident on the upper interface can excite a surface plasmon propagating along the lower (gold–air) interface. When the thickness of Cr layer is zero, the excitation of this surface wave is accompanied by a sharp minimum in the reflectivity (see later; figure 2) with a value depending on the Au thickness. The existence of a Cr layer can drastically modify the system response so that a maximum is observed instead of a minimum (see later; figure 3). In a recent paper [2] Bussjager and Macleod called this observation 'completely unexpected' and correctly pointed out its connection with the high absorption losses of the Cr layer.

Our aim in this paper is to go further towards a quantitative explanation. Using the phenomenological approach well-known in the theory of grating resonance anomalies, it is possible to completely determine the system response using only a few parameters, namely the pole and the zero(s) of the scattering operator. This approach has proved to be powerful in explaining and predicting the peculiarities of grating anomalies in both linear and nonlinear optics [3–5]. Moreover, it gives a natural unification of the cases with minima or maxima in the reflectivity, because in the grating studies both 'normal' and 'inverted' resonances (in the context of references [1] and [2]) are equally frequent and usually exist together.

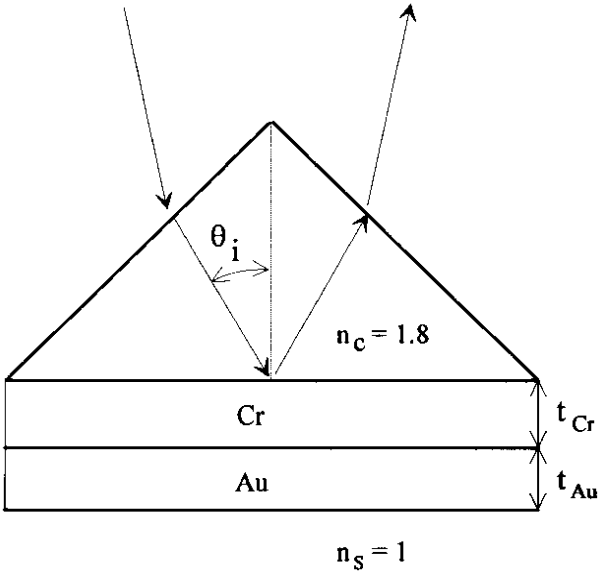

Figure 1. Schematic representation of a prism coupler with two different metallic layers deposited on the prism's large facet. TM polarization, wavelength 632·5 nm. Prism optical index $n_c = 1{\cdot}8$, optical index of Cr: $n_{Cr} = 3{\cdot}55789 + i\,2{\cdot}83876$, and of Au: $n_{Au} = 0{\cdot}23783 + i\,3{\cdot}384755$.

The maximum can be hidden in otherwise high reflectivity conditions and can be clearly observed when the background is low.

2. Guided waves and reflection anomalies: the phenomenological approach

The basic ideas of the phenomenological approach go back to the work of Fano in 1941 [6]. Hessel and Oliner [7] contributed to the physical understanding of grating anomalies from a phenomenological point of view. This was followed by several reviews by Neviere [8], Maystre [3] and Popov [4].

Surface (guided) wave definition requires that there exist scattered fields without incident waves. This definition immediately points to a solution of a *homogeneous* scattering problem, which exists only if there is a pole of the scattering operator of the system. Let us define the scattering problem as follows. One (or several) electromagnetic waves may be incident on the scattering system. We will assume their number to be N and their amplitudes to a_n, $n = 1, \ldots, N$. Column vector $\mathbf{A}$ will contain $\{a_n\}$ as components. These incident waves generate N scattered waves of type and direction determined by the systems optogeometrical parameters. For a flat slab, the scattered waves are simply the reflected and transmitted waves. Their amplitudes are denoted by b_n, which form a column vector $\mathbf{B}$. In linear optics, $\mathbf{A}$ and $\mathbf{B}$ are connected through a linear operator $\mathscr{S}$ called the system scattering operator and represented by a square matrix $\mathbf{S}$ so that:

$$\mathbf{B} = \mathbf{S}\mathbf{A}. \tag{1}$$

It is useful to define another matrix $\mathbf{M}$ which is the inverse of $\mathbf{S}$:

$$\mathbf{M} = \mathbf{S}^{-1}, \tag{2}$$

because usually in numerical studies the solution of the scattering problem is found by solving a linear set of algebraic equations:

$$\mathbf{M}\mathsf{B} = \mathsf{A}. \tag{3}$$

Solution of the homogeneous problem (or equally the existence of a guided wave) requires that equation (3) has a non-zero solution for B without incident fields:

$$\mathsf{A} = 0. \tag{4}$$

This is possible if only the determinant of $\mathbf{M}$ is null:

$$\det(\mathbf{M}) = 0, \tag{5}$$

i.e. the determinant of the scattering matrix $\mathbf{S}$ has a pole. Usually the system parameters are fixed so that the solution of equation (5) is searched as a function of the horizontal component k_x of the wavevector k. It is also convenient to introduce a normalized value

$$\alpha = k_x/|k|, \tag{6}$$

called ' propagation constant'. Then, in the close vicinity of the solution of equation (5), the determinant of $\mathbf{M}$ can be represented through its first term in the Taylor series:

$$\det(\mathbf{M}) = q(\alpha - \alpha^{\mathrm{P}}), \tag{7}$$

where α^{P} is the exact solution of equation (5):

$$\det[\mathbf{M}(\alpha^{\mathrm{P}})] = 0. \tag{8}$$

As an obvious consequence of the link between $\mathbf{S}$ and $\mathbf{M}$ (equation (2)) one immediately finds that

$$\det[\mathbf{S}(\alpha)] = c/(\alpha - \alpha^{\mathrm{P}}), \qquad c = 1/q, \tag{9}$$

so that α^{P} is a pole of the determinant of $\mathbf{S}$ and thus of all its components.

Strictly speaking, for prism coupler, the existence of a guided wave requires that the propagation constant is greater than the optical indices of the cladding n_{c} and the substrate n_{s}:

$$\alpha^{\mathrm{P}} > \max(n_{\mathrm{c}}, n_{\mathrm{s}}), \tag{10}$$

so that the electromagnetic field of the guided wave is evanescent both in the cladding and substrate. The metal–dielectric boundary supports a guided wave called a surface plasmon when $\mathrm{Re}(n_{\mathrm{M}}^2) < -\mathrm{Re}(n_{\mathrm{D}}^2)$ only in TM (or p, or S) polarization, where M denotes the metal and D the dielectric. The propagation constant of the plasmon is simply equal to:

$$\alpha^{\mathrm{P}} = n_{\mathrm{D}}^2/(n_{\mathrm{D}}^2 + n_{\mathrm{M}}^2)^{1/2}. \tag{11}$$

For highly conducting metals, the real part of the plasmon propagation constant is slightly greater than the optical index of the dielectric and its imaginary part depends on the metal absorption. In the prism coupler, there are normally two surface plasmons: one on the lower boundary and one on the upper. Their propagation constants are $\alpha_{\mathrm{s}}^{\mathrm{P}}$ and $\alpha_{\mathrm{c}}^{\mathrm{P}}$ respectively. When the metal thickness is large, these two plasmons are the plasmons propagating along the semi-infinite metallic

surface coated with the corresponding dielectric. It immediately follows from equation (11) that the second (upper interface) plasmon cannot be excited through the plane wave incident on the prism because

$$\mathrm{Re}\,(\alpha_c^P) > n_c, \tag{12}$$

and Snell's law requires phase matching between the incident and the surface wave:

$$\alpha(\equiv n_c \sin\theta_i) = \mathrm{Re}\,(\alpha^P). \tag{13}$$

The plasmon propagating on the lower (metal–air) boundary can be excited through the prism when the metal is thinner, so that coupling is provided between the incident wave and the evanescent field of the guided wave. In this case, the plasmon is not a guided wave, strictly speaking, because it can be radiated in the cladding. The finite thickness of the metal modifies the plasmon propagation constant. One of the obvious effects is the increase of its imaginary part because the radiation losses in the cladding are added to the absorption losses in the metal. The other direct consequence is that the reflected wave amplitude has a pole in the vicinity of the plasmon excitation. This can be immediately found by substituting equation (9) into equation (1)):

$$b_1 = a_1 c_{11}/(\alpha - \alpha^P). \tag{14}$$

This equation is valid for any metal thickness and, in particular, when the thickness increases to infinity. However, in the latter case there is no resonance anomaly in the reflectivity. On the other hand, the amplitude of the reflected wave is always limited—it can never exceed the incident wave amplitude. This means that equation (14) is not sufficient to adequately determine the system response in the resonance region. When the metal thickness increases, the numerator of equation (14) has to compensate the pole, i.e. the numerator must have a zero α^z. Direct evidence can be found by taking into account a second term in representation (14):

$$b_1 = a_1\left[\frac{c_{11}}{(\alpha-\alpha^P)} + \frac{\hat{c}_{11}}{(\alpha-\alpha^P)^2}\right] \equiv a_1 c_{11}\frac{(\alpha-\alpha^P+\hat{c}_{11}/c_{11})}{(\alpha-\alpha^P)}. \tag{14a}$$

Thus the numerator is nul when $\alpha = \alpha^P - \hat{c}_{11}/c_{11}$ and one arrives at the final form of the phenomenological formula:

$$b_1 = r_0 a_1(\alpha-\alpha^z)/(\alpha-\alpha^P), \tag{15}$$

where r_0 is the reflectivity of the system without the plasmon excitation. When the metal thickness increases, the pole and the zero tend to merge together so that the anomaly disappears (see later, figure 4).

There is another way of deriving equation (15). In fact, the resonance response (equation (14)) must be added to the non-resonance system reflectivity r_0 which is not zero even without the plasmon excitation, so that equation (14) must be rewritten as

$$b_1 = a_1[r_0 + c_{11}/(\alpha-\alpha^P)], \tag{16}$$

which immediately leads to equation (15) with

$$\alpha^z = \alpha^P \times c_{11}/r_0. \tag{17}$$

The zero, like the pole, is, in general, complex, but for some system parameters

its imaginary part can become null so that the reflectivity minimum can become zero for real angles of incidence.

If the anomaly is single, the pole and the zero, as well as r_0, depend only slightly on the incident angle. The validity and the usefulness of equation (15) have been demonstrated in the studies of grating anomalies. Numerical codes that are made to determine the reflection (and transmission) have to be generalized to work in the complex plane of wavenumbers and have to be incorporated in a root-finding procedure. In fact, the numerical results presented in this paper were obtained using a code devoted to the study of multilayered gratings. This code can be directly applied to a prism coupler by simply stating that the groove depth is equal to zero.

3. The 'normal' and the 'inverted' resonances

The validity of the phenomenological formula (equation (15)) can be observed in figures 2 and 3 where the rigorous results for both the 'normal' and the 'inverted' resonances are compared with the predictions of equation (15). It is obvious that a simple change of the values of the pole and the zero converts the 'normal' resonance into an 'inverted' one. As already mentioned, it is possible to identify the anomaly by tracing the pole and the zero when increasing the thickness of Au layer. This is much safer than tracing the position of the maximum in the reflectivity because it does not always correspond to the plasmon propagation constant, as demonstrated later. Figure 4 represents the dependencies of the real and imaginary part of the pole and the zero on the Au layer thickness without a Cr layer. Above a particular thickness (about 100 nm), the zero and the pole merge together so that no anomaly is observed. The limit of α^p corresponds to the propagation constant of a plasmon along the bulk Au–air interface. Below, say, 100 nm, the coupling between the incident field in the prism and the plasmon at

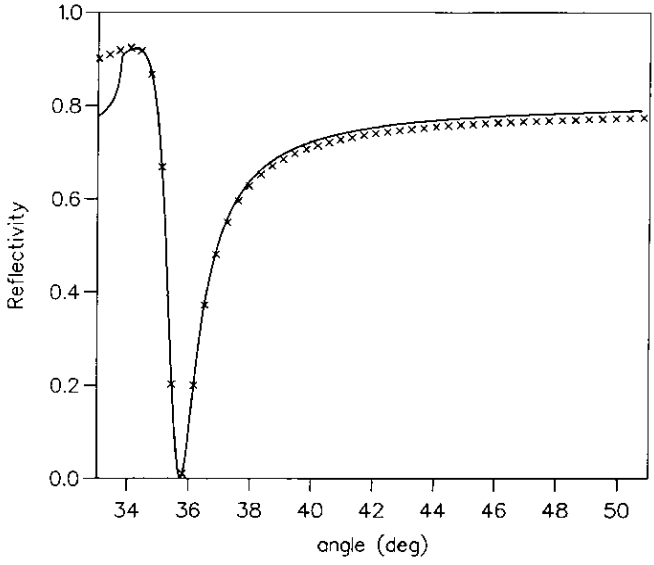

Figure 2. Reflectivity of prism coupler shown in figure 1 with a single gold layer. $t_{Cr} = 0$, $t_{Au} = 45$ nm. Solid line—rigorous numerical results, crosses—results using equation (15) with $r_0 = 0{\cdot}8$, $\alpha^p = 1{\cdot}045575 + i\,0{\cdot}01417216$, and $\alpha^z = 1{\cdot}051165 + i\,0{\cdot}0000321$.

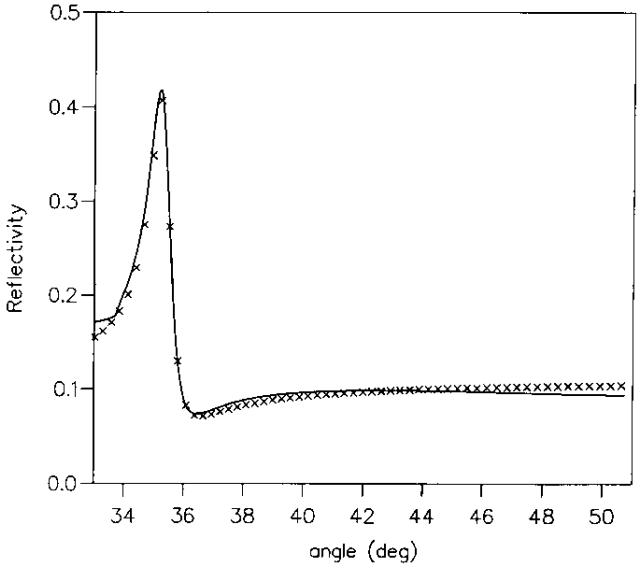

Figure 3. As in figure 2 except that $t_{Cr} = 15$ nm. $r_0 = 0{\cdot}11$, $\alpha^p = 1.042015 + i\,0{\cdot}010792$, $\alpha^z = 1{\cdot}052573 + i\,0{\cdot}01669$.

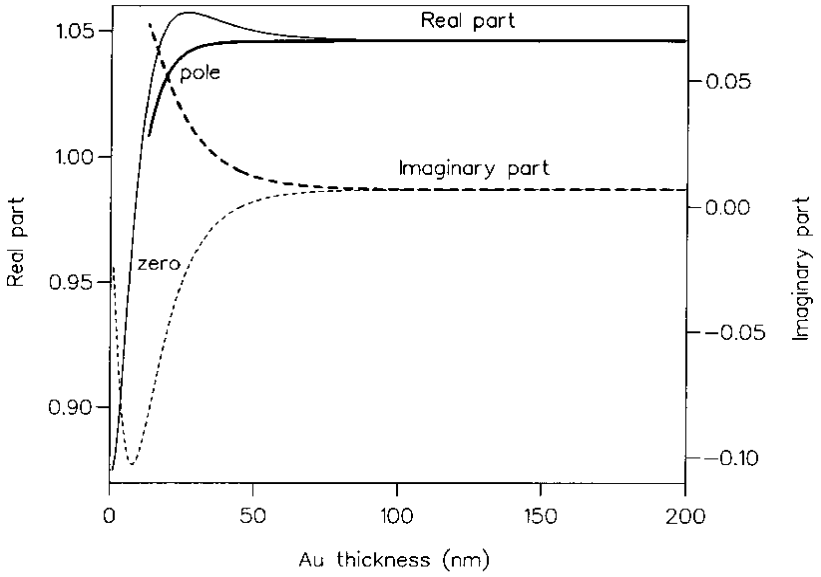

Figure 4. The real and imaginary parts of the pole and the zero as a function of t_{Au}, $t_{Cr} = 0$.

the lower interface increases and so does the imaginary part of the pole, due to the increase in the radiation losses of the plasmon in the cladding. The imaginary part of the zero goes in the opposite direction. This fact can be explained by taking into account the high conductivity of Au. When the layer is perfectly conducting, it can be demonstrated rigorously, using the energy conservation, that the pole

and the zero are complex conjugated, so that equation (15) will always lead to a reflectivity equal to unity. The finite conductivity of Au breaks the exact symmetry but does not change qualitatively the behaviour (as can be observed later in figure 7): the imaginary part of the pole increases and the imaginary part of the zero decreases with t_{Au}. As a consequence, for some value of t_{Au} (45 nm), the zero becomes real and the prism coupler can totally absorb the incident light at a suitable angle of incidence:

$$\alpha \equiv n_c \sin\theta_i = \mathrm{Re}\,(\alpha^z). \tag{18}$$

Further decreases of the layer thickness moves the zero below the real axis so that the minimum value of the reflectivity grows.

It must be pointed out that, depending on the relative position of the pole and the zero, the system can exhibit a variety of responses. When the zero is closer to the real axis, a sharp minimum is observed, which can be accompanied by a maximum if the real parts of the pole and the zero differ, as it is the case with figure 2. The maximum is shifted from the pole as can be clearly observed in figure 5(*b*). When a Cr layer is introduced, the imaginary part of α increases (figure 6) where $\mathrm{Re}\,(\alpha^p)$, $\mathrm{Im}\,(\alpha^p)$, and $\mathrm{Re}\,(\alpha^z)$ do not move significantly (see figures 5 (*b*) and 6). As directly follows from equation (15), this will lead to an increase of the minimum in the reflectivity. Also, the maximum moves closer to the real part of the pole (upper part of figure 5 (*b*)). As the total absorption losses increase with Cr thickness, the value of the maximum decreases (figure 5 (*a*)).

The influence of the Cr layer can be more easily observed in figure 7, which presents the trajectories of the pole and the zero in the complex α-plane as a function of Au thickness for four different values of t_{Cr}. The starting point at $t_{Au} = 200$ nm corresponds to a virtually infinite thickness of Au. Then the zero and the pole merge together, there is no anomaly in the reflectivity and the plasmon properties are not affected by the presence of Cr. Going away from this central point, the Au thickness decreases from 200 nm to 13 nm at the other end of the trajectories. Below that thickness, the real part of the pole becomes less than 1 and the plasmon is cut off. The curves with $t_{Cr} = 0$ have been discussed already and the trajectories of the pole and the zero are most symmetrical, with α^z crossing the real axis at $t_{Au} = 45$ nm, resulting in the reflectivity dependence presented in figure 2. With the increase of Cr thickness, the trajectories of the pole and the zero becomes less symmetrical with respect to the real α-axis. Although the absorption losses increase, the radiation losses of the plasmon in the prism decrease due to the buffering effect of the Cr layer, so that the imaginary part of the pole slightly decreases with t_{Cr}. The behaviour of the zero is more spectacular. Below $t_{Cr} = 10$ nm the trajectory of the zero always crosses the real axis, although at different points of α and t_{Au}. This means that for a suitable Au thickness, total absorption of incident light always exists, the maximum and the minimum being more and more separated. For example, when the Cr thickness is equal to 10 nm, α^z crosses the real axis at $t_{Au} = 19{\cdot}765$ nm and total absorption occurs for $\alpha = 1{\cdot}145$ (figure 7), which corresponds to $\theta_i = 39{\cdot}7^\circ$ (figure 8). Due to the large distance between the pole and the zero, well distinguished maximum can also be observed.

Increasing t_{Cr} (for example, figure 7 with $t_{Cr} = 15$ nm) pushes the trajectory of the zero completely above the real axis so that for any Au thickness the minimum in the reflectivity does not become zero. Moreover, as α^z moves far into the complex plane with the imaginary part exceeding the imaginary part of the pole, the

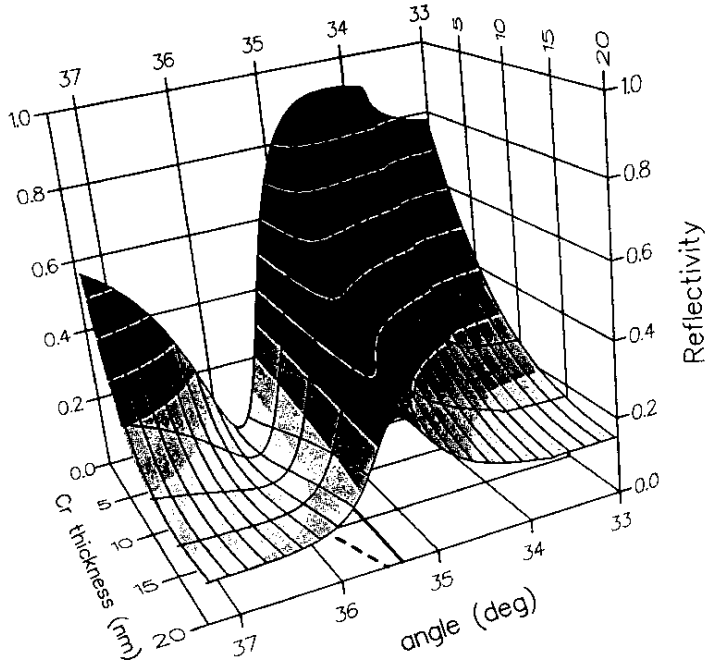

Figure 5. Reflectivity of the prism coupler given in figure 1 as a function of the angle of incidence and t_{Cr}. $t_{Au} = 45$ nm. (*a*) A 3-D view, (*b*) an upper view with the reflectivity isolines and the trajectories of the real part of the pole (solid heavy line P) and the zero (dashed line Z).

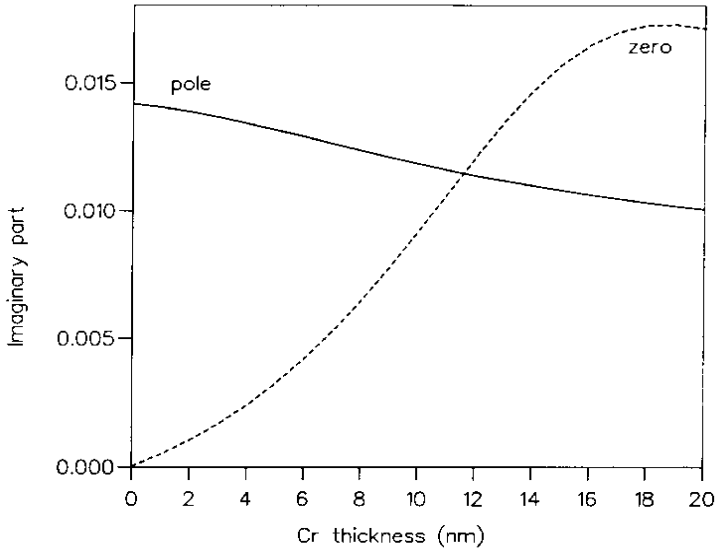

Figure 6. The imaginary parts of the pole and the zero as a function of t_{Cr} for $t_{Au} = 45$ nm.

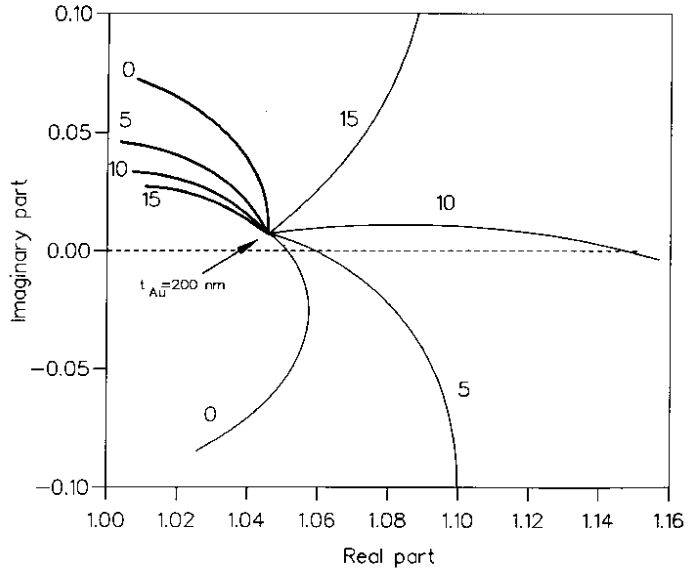

Figure 7. The trajectories of the pole and the zero in the complex α-plane when the gold film thickness is varied from 200 nm at the central point to 13 nm at the end of the curves. Results are presented for four values of t_{Cr} of 0, 5, 10 and 15 nm, as indicated in the figure.

influence of the zero on the reflectivity (which is measurable for real values of α) becomes negligible, as a direct consequence of equation (15). As a result, no minimum in the reflectivity is observed in figure 3. It must be pointed out that the lack of a minimum does not mean that the zero has disappeared—when going

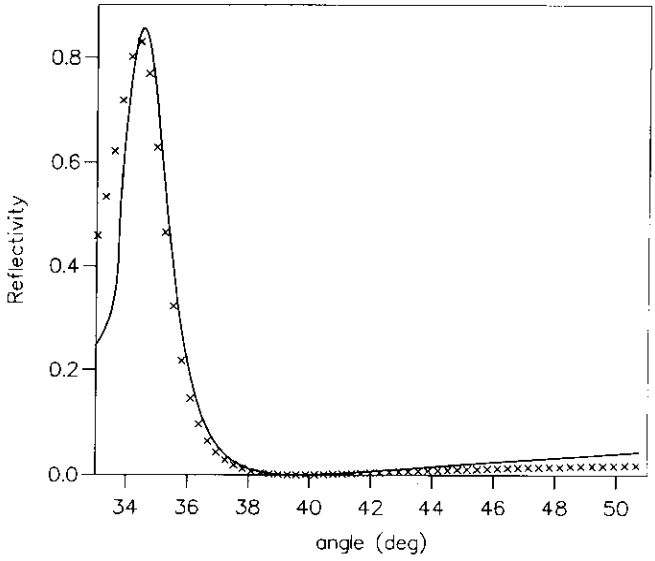

Figure 8. The same as in figures 2 and 3 except that $t_{Cr} = 10$ nm and $t_{Zu} = 19{\cdot}765$ nm. The corresponding phenomenological parameters are $r_0 = 0{\cdot}0425$, $\alpha^P = 1{\cdot}022762 + i\,0{\cdot}02907926$, and $\alpha^z = 1{\cdot}148013 + i\,0{\cdot}0000073$.

from figure 2 to figure 8 and to figure 3, both pole and zero continue to exist, but only their relative position changes.

4. Conclusion

We demonstrate in this paper that a phenomenological approach is capable of a quantitative explanation of both the 'normal' and the 'inverted' resonance curves in the reflectivity of a prism coupler when a surface plasmon is excited. From that point of view, both types of resonances are 'normal' and they differ simply by a change of position of two phenomenological parameters, namely the complex pole and zero of the reflectivity amplitude.

References

[1] Printz, M., and Sambles, J. R., 1993, *J. Mod. Opt.*, **40,** 2095.
[2] Bussjager, R., and Macleod, H. A., 1995, *J. Mod. Opt.*, **42,** 1355.
[3] Maystre, D., 1982, *Electromagnetic Surface Modes*, edited by A. D. Boardman (John Wiley), chap. 17.
[4] Popov, E., 1993, *Progress in Optics*, Vol. XXXI, edited by E. Wolf (North-Holland, Amsterdam: Elsevier), pp. 139–187.
[5] Neviere, M., Popov, E., and Reinisch, R., 1995, *J. Opt. Soc. Am.* B, **12,** 513.
[6] Fano, U., 1941, *J. Opt. Soc. Am.*, **31,** 213.
[7] Hessel, A., and Oliner, A. A., 1965, *Appl. Opt.*, **4,** 1275.
[8] Neviere, M., 1980, *Electromagnetic Theory of Gratings*, edited by R. Petit (Berlin: Springer-Verlag), chap. 5.